Downtime cost analysis of offloading operations under irregular waves in Malaysian waters

M.S. Patel[*1], M.S. Liew[1a], Zahiraniza Mustaffa[1b],
Abdurrasheed Said Abdurasheed[1c] and Andrew Whyte[2d]

[1]Department of Civil and Environmental Engineering, Universiti Teknologi PETRONAS, Perak, Malaysia
[2]Department of Civil and Environmental Engineering, Curtin University, Perth, Australia

Abstract.   The objective of this study was to evaluate the downtime cost of side-by-side offloading operations in Malaysian waters. With the help of a numerical time domain tool, the structure and cable response of moored FPSO vessel was simulated for heading and beam sea-states under irregular waves. The weather downtime was assessed by comparing the response under operational wave condition with the pre defined industrial safe offloading criteria. Additionally, two cases of cable failure were simulated for each sea-state. The novel study on downtime cost was presented for three different location of Malaysia subcontinent for which the location specific wave scatter diagram facilitated to estimate the probability of occurrence of operational wave condition. It was concluded that an unpredictable increment in wave height by 0.5 m can significantly impact the production cost.

Keywords: floating bodies; hydrodynamics; irregular waves; mooring; downtime; offloading, mooring

1. Introduction

A recent survey on floating production storage and offloading (FPSO) systems revealed a total of 178 FPSOs working around the globe (Mahlstedt and Davis 2017), 14 FPSOs are currently operating in Australian waters while 51 FPSOs are stationed in Southeast Asia. Malaysia alone has 6 FPSOs, as shown in Fig. 1. Side-by-side offloading operations are preferable for offloading crude oil in mild weather conditions. This involves the positioning of shuttle tanker on either side of FPSO. On the other hand, tandem offloading operations are usually employed in harsh weather conditions. This requires a shuttle tanker to be positioned in line with aft/fwd of the FPSO. The side-by-side configuration is of recent origin and more preferred because of stability and lower cost of production. The safety of operations is dependent on the hydrodynamic forces. The approach of evaluating the motion responses and cable forces in maximum operational environments have limitations (Cueva

---

and Tannuri 2009). In an event of high weather conditions or failure of certain component of operating vessel, downtime may occur (Shihab *et al.* 2020). This downtime affects the production and global economy overall. This paper deals with estimating the downtime cost of offloading operations either due to excursion of motion response and cable forces or failure of mooring cable. A downtime cost study in two sea-states for different offloading capacities of shuttle tankers was presented. A time domain numerical package was employed to evaluate the motion response and cable forces under different operational wave conditions. This paper has been divided into six sections. Section 2 surveys the past work performed and presents the background of study. The methodology, numerical formulations including geometric modeling of vessels is presented in Section 3. Section 4 presents the time domain results of structure position and cable forces including the results due to mooring failure. The downtime cost analysis is presented in Section 5. Section 6 concludes the study and briefly summarizes the present study and scope for future work.

2. Background

The background comprises of both hydrodynamic interaction and downtime studies performed in the past. Time domain simulations were conducted by (Lee *et al.* 2017) to predict the hydrodynamic response for submerged floating tunnel under wave and seismic excitations. (Corrêa *et al.* 2013) presented a methodology based on static calculation of dynamically positioned vessel for determining the downtime of offloading operations. The mathematical modeling consisted of static analysis where mean forces are calculated without considering the dynamic effects. (Buchner *et al.* 2001) developed and validated a numerical model for prediction of relative motions and mooring loads during side-by-side offloading operations. In those analysis, only waves were considered as environmental forces. The research paper by (Zhao *et al.* 2018) highlighted the key parameters that determine the offloading feasibility. One of the factors are roll motions and gap between vessels. The authors have also specified side-by-side offloading to be a preferred method of offloading as compared to tandem offloading practice. Numerical simulations based on higher order formulations were used to investigate the mooring dynamics and hull motions under irregular waves (Kim and Kim 2016). Hydrodynamic interaction for side-by-side configuration using higher order numerical methods was presented in (Hong *et al.* 2002). The feasibility of offloading of FLNG into a carrier is studied from long term data sets of three locations (Ewans and Jameson 2015). The environmental data sets are of prime importance to assess the design and operation in open oceans. Furthermore, the hindcast data supported these requirements. The operational window where significant wave height is less than critical specified value was estimated. The hind cast data of the three locations provided the operational window and waiting time was calculated. A time domain coupled analysis code, `SIMO', was employed to numerically simulate the hydrodynamic performance of multiple bodies in close proximity by (Zhao *et al.* 2012). The research paper by (Zhao *et al.* 2014) have studied hydrodynamic characteristics for two floating vessels and their structural components through a time domain numerical program. A smart offloading system for LNG was proposed by (Paquet *et al.* 2016), which used proven technology as opposed to conventional carriers. Technical descriptions of the system were explained along with several real time numerical simulations in different environmental conditions were carried out to assess the capability of the offloading system. The risk assessment of side-by-side offloading configuration has been studied under different environment conditions within operating sectors. The side-by-side offloading operation throughout the world were presented in (Poldervaart *et al.* 2006), and

alternative offloading possibilities were discussed for locations where higher uptime was required. A study was presented on the factors affecting the motion response and cost was identified through system thinking approach (Nishanth 2018). A downtime cost study was performed by (Patel *et al*. 2020) to evaluate the downtime cost of offloading operations due to influence of parametric rolling of shuttle tanker.

The research paper (Morandini *et al.* 2002) discussed time domain tools through which specific criteria for offloading operations can be assessed. The authors (Van Doorn and Ten Hove 2002) studied economic performance of a vessel which was affected by weather downtime. They also presented tools which were available for numerical simulations. Eventually, the authors focused on the combination of numerical tools with experience for safe offloading operations. A safe offloading assessment under limiting environmental conditions with more attention towards risk of collision was discussed. The downtime condition considered was extreme environmental conditions, failure of engine, gear and tugs. For each downtime simulation, the risk of collision was observed. Furthermore, Quantitative Risk Assessment was studied under which possible scenarios were found where possibility of collision could occur. A numerical model to provide evaluation and testing of dynamically positioning system for a FPSO and shuttle tanker during offloading was presented in (Peng and Spencer 2008). A new method to determine the storage capacity for side-by-side offloading operation has been proposed by researchers (Kessel-cobelens *et al.* 2008). The proposed methodology is based on model testing for past 10 years environmental data. Navigation simulation has been used to determine the offloading criteria. Furthermore, cost analysis was performed for the FLNG to determine the inventory and production costs. Finally cost benefit analysis using Net Present Value (NPV) methods allowed to decide the suitability of FLNG storage capacity. The downtime analysis was based on availability of offloading window. An uncoupled dynamic analysis was performed in a numerical software where in the operating conditions for the dynamic analysis was similar to Malaysian field (Nishanth *et al*. 2016).

The operational envelopes of wave kinematics including shear forces and bending moments were obtained for submerged floating tunnel under extreme irregular wave conditions (Jin and Kim 2017). (Jin and Kim 2017) have demonstrated time domain simulation for different mooring lines. A numerical wave model was employed for determining the significant wave height at each port of consideration in (Dqg *et al.* 2017). The validation of the numerical results was performed with the wave measurements by oceanic buoys. Operability envelopes were computed in (Chang *et al*. 2014), by modeling the structural element as finite number of beam elements and solving for a finite element formulation. The research paper (Ballard and Evans 2014) have presented the total time required for completing operation by considering the weather conditions which limit the connected sequential task to the main operation. A case study was presented where operational costs were minimized by facilities improvement and low-cost alternatives. The successful implementation of keeping both OPEX and CAPEX less with safety and integrity in the plan was the breakthrough for redevelopment of field (Lim *et al.* 2015). A technique to inspect the events responsible for downtime of operation of fishing vessel was presented in (Pillay *et al.* 2001). A delay time parameter estimation has been proposed to minimize the occurrence of downtime due to unexpected failure of equipment on the vessel. A downtime analysis of a shuttle tanker with and without dynamic station keeping was presented in (Cueva and Tannuri 2009), where the results of the study has been summarized as percentage of occurrence per year. The economical risks and uncertainties involved in offloading operations in Malaysian waters were evaluated by (Patel *et al*. 2019). With the past works on the topic of operability and downtime, it has been observed that no much work has been done in estimating the downtime cost due to motion responses and failure of structural components.
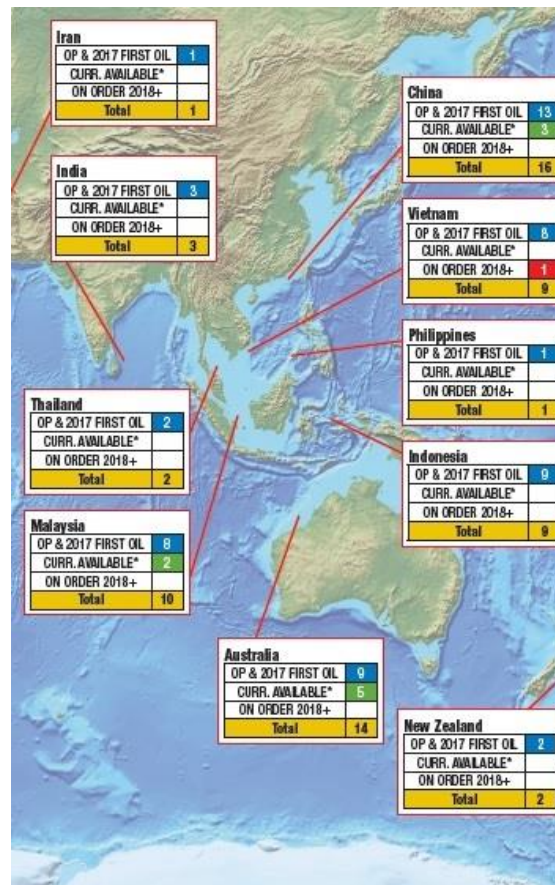
Fig. 1 South East Asia and Australia distribution of FPSO (Source: Offshore magazine, August 2017)

The objective of this study is to evaluate the downtime cost of offloading operations due to structure response and mooring failure.

3. Methodology and modelling

This study on calculating the downtime cost in Malaysian water of finite water depth of 100 m was limited to three different locations. The numerical time domain tool, `ANSYS AQWA' was used to evaluate the motion responses and cable forces in irregular waves. The time domain numerical tool `ANSYS AQWA' is a complete integrated hydrodynamic analysis package based on three-dimensional diffraction and radiation theory. The moored FPSO and shuttle tanker were modelled and analysed for safe and operational wave conditions. The predetermined motion response and cable forces under safe wave criteria allowed to calculate the downtime under operational wave conditions. The three locations of interest represent different working domain in Malaysian subcontinent. The hindcast sea fine data for each location of interest was obtained. The locations are renamed to protect the privacy of the met-ocean data. The source distribution method

which is employed in the numerical time domain tool describes the fluid structure interaction by set of equations in fixed reference axes as following

$$\Delta\phi = \frac{\partial^2\phi}{\partial X^2} + \frac{\partial^2\phi}{\partial Y^2} + \frac{\partial^2\phi}{\partial Z^2} \tag{1}$$

$$\frac{\partial\phi}{\partial n} = -i\omega n_j \tag{2}$$

$$\frac{\partial\phi}{\partial n} = -\frac{\partial\phi}{\partial n} \tag{3}$$

Eq. (1) is the Laplace equation while Eqs. (2) and (3) are the body surface conditions. An additional equation is needed so that the disturbance dies out, which is known as radiation condition as shown in Eq. (4).

$$\sqrt{x^2 + y^2} \longrightarrow \infty \tag{4}$$

The Green's function in the certain finite depth is a frequency domain mathematical expression which is introduced to solve the velocity potential through boundary integration technique. The Green function is represented in the following Eq. (5).

$$G(X,\zeta,\omega) = \frac{1}{r} + \frac{1}{r_2} + \int_0^\infty \frac{2(k+v)e^{kd}\cosh[k(Z+d)]\cosh[k(\zeta+d)]}{k\sinh(kd)-v\cosh(kd)} J_0(kR)dk +$$
$$i2\pi \int_0^\infty \frac{(k_0+v)e^{k_0 d}\cosh[k_0(Z+d)]\cosh[k_0(\zeta+d)]}{\sinh(k_0 d)+k_0 d\cosh(k_0 d)-vd\sinh(k_0 d)} \tag{5}$$
$$J_0(k_0 R)dk$$

where,

J_0 is the Bessel function of first kind

$v = \frac{\omega^2}{g}$

$R = [(X-\zeta)^2 + (Y-\eta)^2]^{\frac{1}{2}}$

$r = [R^2 + (Z-v)^2]^{\frac{1}{2}}$

$r_2 = [R^2 + (Z+v-2d)^2]^{\frac{1}{2}}$

The following condition should be satisfied in the fluid field

$$\Delta G(X,\zeta,\omega) = \frac{\partial^2 G}{\partial X^2} + \frac{\partial^2 G}{\partial Y^2} + \frac{\partial^2 G}{\partial Z^2} = \delta(X-\zeta) \tag{6}$$

With the aid of Green's theorem, the velocity potential satisfying the body surface conditions are then expressed as Fredholm's integral equation of second kind. These integral equations are solved by constant panel method. The AQWA-NAUT module was used to simulate the real time motion of geometrically modelled FPSO in side-by-side configuration with a shuttle tanker. The acceleration impulse function defined by Eq. (7) is employed in the equation of motion for converting the frequency domain to time domain. ANSYS AQWA implements new damped free surface boundary by extending widely used wave-absorbing beach method. This is done to suppress unrealistic

resonant wave oscillation which occurs due to absence of viscous flow effects in potential flow diffraction and radiation calculation.

$$h(t) = \quad -\frac{2}{\pi}\int_0^\infty B(\omega)\frac{\sin(\omega t)}{\omega}d\omega = \frac{2}{\pi}\int_0^\infty A(\omega) - \quad A_\infty \cos(\omega t)\,d\omega \qquad (7)$$

3.1 Geometric modeling

The designer modeler interface in `ANSYS AQWA' facilitates to input the geometrical details of the FPSO and shuttle tanker. The vessels are placed in a side-by-side configuration as shown in Fig. 2. The geometric details of the vessel are shown in Table 1. The response of FPSO and cables were analysed for irregular waves in head and beam sea-states. For each sea-state, the safe offloading criteria wave condition was obtained from PETRONAS oil company. The response under the safe offloading criteria was predetermined and kept as a benchmark for offloading operations. Additionally, the response of vessel structure and cable was also analysed under operational wave condition.

Table 1 Geometric details of FPSO and shuttle tanker

Category	Detail	FPSO	Shuttle Tanker
	Length (m)	182.84	151.60
	Beam (m)	32.2	25.9
	Total Depth (m)	19.55	17.24
Geometric details	Total structural mass (kg)	58.25e6	23.46e6
	K_{xx} (m)	10.948	8.806
	K_{yy} (m)	45.71	37.9
	K_{zz} (m)	47.54	39.4
	I_{xx} (kg-m^2)	69.82e8	18.19e8
	I_{yy} (kg-m^2)	12.17e10	33.7e9
	I_{zz} (kg-m^2)	13.16e10	36.45e9
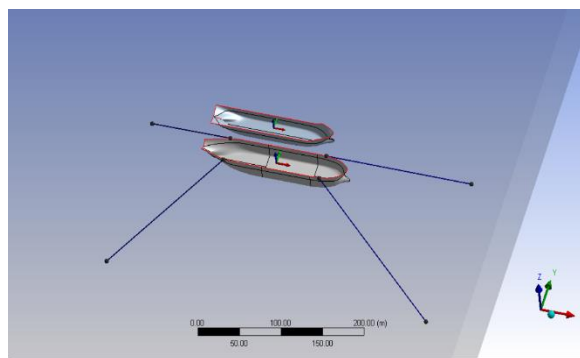
Fig. 2 FPSO and shuttle tanker

Table 2 Mooring details of FPSO

Cable	Description	Details
1	Fair lead coordinates	(30,15.5,5.5)
	Anchor coordinates	(-100, 100, -100)
	Stiffness (N)	6000000
	Length (m)	187.53
2	Fair lead coordinates	(30, -15.5,5.5)
	Anchor coordinates	(-100, -100, -100)
	Stiffness (N)	6000000
	Length (m)	187.53
3	Fair lead coordinates	(150,16.1,5.5)
	Anchor coordinates	(300, 100, -100)
	Stiffness (N)	6000000
	Length (m)	201.66
4	Fair lead coordinates	(150, -16.1, 5.5)
	Anchor coordinates	(300, -100, -100)
	Stiffness (N)	6000000
	Length (m)	201.66

3.2 Mooring details

The FPSO was spread moored and the cables considered were linear elastic for which the specifications were obtained from experts in offshore industry. Table 2 displays the details of mooring for the FPSO considered for time domain hydrodynamic analysis. The response of mooring cables were also studied under operational wave conditions. Two cases of mooring failure were simulated. The first was due to single point of time failure and the second was due to tension exceedance. The single point of time failure included the cable to fail at certain interval of time due to non-functioning of the mooring cable. The ultimate objective was to calculate the downtime cost due to failure of mooring cables. Therefore, the exact reasons of cable failure are beyond the scope of present study. The second kind of failure is when the tension in the cable exceeds the predefined tension.

The predefined tension was calculated under safe offloading wave conditions. In the present study, the representation of each case of mooring failure is highlighted once. The single point of time failure is simulated under head seas while failure due to tension exceedance is simulated under beam seas, respectively.

3.3 Location of interest

The Malaysian subcontinent has many FPSOs working in the present scenario. Three locations of them are chosen to study the downtime cost for offloading operations. The hind cast data for these locations are collected from Offshore Engineering Centre (OEC), Universiti Teknologi PETRONAS, Perak, Malaysia. With the aid of available hind cast data, the wave scatter diagrams was prepared. The wave scatter diagram of each location would facilitate to provide the probability of occurrence for the required wave condition. The wave scatter for locations 'B' and 'C' were derived in the same manner but only wave scatter for location 'A' is presented in Table 4.

3.4 Downtime cost analysis

The industrial practice of offloading is by studying the weather prior for 3 days. In an event, when the wave conditions are not within the safe offloading criteria, offloading does not take place. The idea of this research is to possibly calculate the downtime cost when the operational wave conditions exceed the safe offloading criteria. The downtime cost for offloading operations was either due to excessive motion or cable response obtained under operational wave conditions. The excursion of motion or cable response was determined from the values under safe offloading criteria. The downtime was also calculated for failure of mooring cables. Due to any event where downtime occurs, the offloading operation is stopped, and the global economy of the project is affected. The downtime cost is a function of operating expenditure (OPEX), probability of occurrence of wave conditions, duration of downtime and production capacity. The downtime cost is calculated from Eq. (8).

$$z = a \times b \times c \times d \tag{8}$$

where, 'z' represents downtime cost, 'a' represents probability of the occurrence of wave condition, 'b' is downtime duration, 'c' is OPEX and 'd' is the production capacity.

The downtime cost analysis was based on four different offloading capacity of the shuttle tanker. The offloading capacity is usually less than the production capacity of FPSO. The offloading capacity considered in this study was limited to 70%, 80%, 90% and 100% of the production of FPSO. Also, the OPEX is location specific and varies with respect to many factors. The OPEX considered is US\$ 35 per barrel of oil for all the three locations in Malaysian waters. The OPEX considered is arbitrary and does not reflect any specific operator. However, actual downtime cost can be calculated if OPEX is known for actual offshore site.

4. Results and discussion

The FPSO and shuttle tanker in side-by-side configuration were simulated in irregular waves for two sea-states. The structural motion response of FPSO and whole cable responses were studied under operating and safe criteria wave conditions. The comparison between the peak values of motion response and cable response under head and beam seas are presented. The wave conditions are presented in Table 3. There are two operating conditions considered for head seas. The PM spectrum was used for the simulation of irregular waves. Additionally, PM spectrum is recommended by PETRONAS Technical Standards (PTS). The PM spectrum for safe offloading criteria and operational wave conditions in beam sea-state are shown in Fig. 3. Although, there are two operational wave conditions in heading sea, the PM spectrum is only presented for the first operational wave condition as displayed in Fig. 4. The safe limits which are predetermined under the safe offloading criteria may have small limits but, these are industrial standard for permissible offloading criteria in Malaysian waters. The excursion of the stationed vessels are determined by making a comparison between the limiting values and possible downtime is studied. The figure for the structure and cable response under 'operational wave condition 2' (H_s=2 m and T_p=7.0 s) in head seas has been included in the appendix at the end of the paper.

4.1 Structure response

The FPSO was observed for its structure position under safe criteria wave condition and operational wave conditions. The response of FPSO structure position in beam sea under safe offloading criteria wave condition is shown in Figs. 5 and 6. Figs. 7 and 8 are the structure response under operational wave conditions in beam sea. The response of FPSO under safe offloading criteria and operational wave conditions in head seas are shown in Figs. 9 to 12.

A comparison of the peak values under both wave conditions have been tabulated in Table 5. In beam seas, there is marginal increase in the surge position. A good amount of peak increment is observed under sway and heave positions. Also, rotational positions have significant increase in roll

(a)

(b)
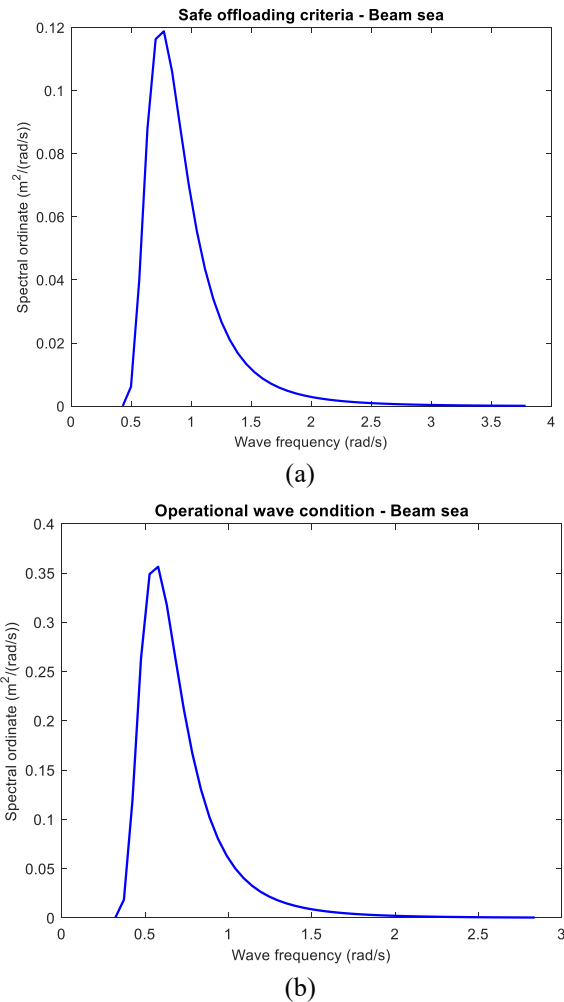
Fig. 3 (a) PM spectrum for beam sea and (b) PM spectrum for beam sea

Table 3 Wave conditions for offloading operation

Sea-state	Safe offloading criteria	Operating condition 1	Operating condition 2
Beam sea	$H_s = 1$ m and $T_p = 6.0$ s	$H_s = 1.5$ m and $T_p = 7.0$ s	-
Head sea	$H_s = 2$ m and $T_p = 6.0$ s	$H_s = 2.0$ m and $T_p = 7.0$ s	$H_s = 2.5$ m and $T_p = 7.0$ s

(a)

(b)
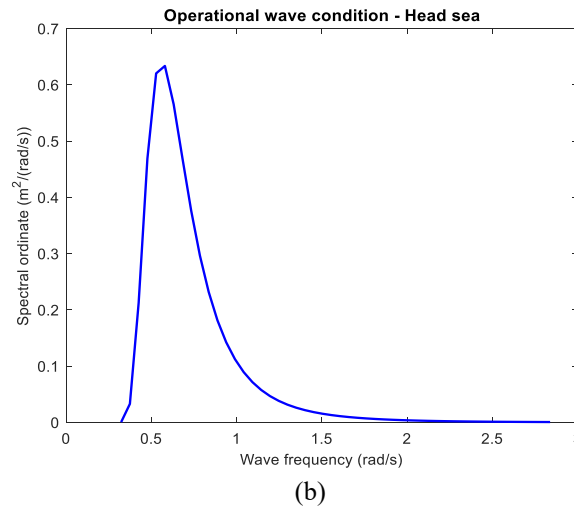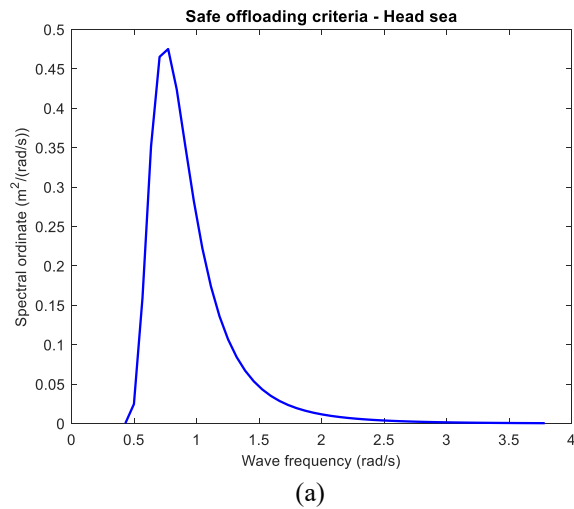
Fig. 4 (a) PM spectrum for head sea and (b) PM spectrum for head sea

whereas pitch and yaw positions are less affected. In head seas, the surge translations are impacted to a good amount. The peak sway translations are not of much significance, but heave positions also show good increase in the peak value. The pitch rotations are much affected as compared to roll and yaw motions. Since the structure positions under operational wave conditions exceed the limiting

values obtained under safe offloading criteria, offloading is ceased and downtime of offloading occurs.

4.2 Cable response

The whole cable tensile forces were calculated for beam and head seas. The values corresponding to safe offloading criteria and operational conditions are presented in Table 6. It is observed from Table 6 that peak whole cable tensile forces significantly increase under the operational wave conditions. The whole cable tensile response in the beam seas are shown in Figs. 13 to 16. Figs. 17 to 20 displays the whole cable tensile forces under first operational wave condition in head sea. There is significant increase in the whole cable forces under operational condition and as they exceed the limiting values of safe offloading criteria, a downtime of offloading operations occurs.
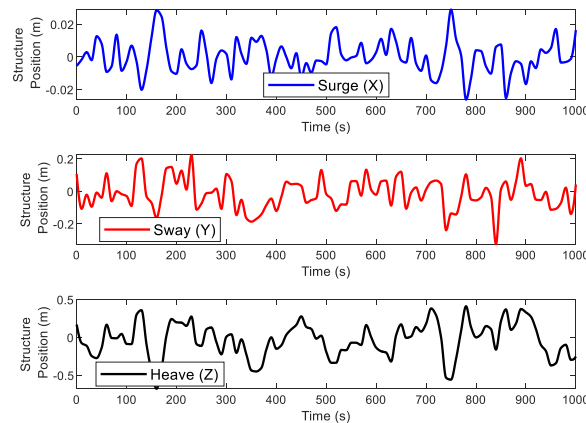
Fig. 5 Structure position (beam sea) - safe offloading criteria

Table 4 Wave scatter for location 'A'

Hs/Tp	0 TO 2	2 TO 4	4 TO 6	6 TO 8	8 TO 10	10 TO 12	12 TO 14	14 TO 16	16 TO 18	TOTAL
0-0.5	32	17,085	179,156	11,116	1,217	393	134	31	14	209,178
0.51-1	0	969	83,187	72,896	2,660	803	320	115	7	160,957
1.1-1.5	0	2	2,382	59,066	4,236	7	6	2	0	65,701
1.51-2	0	0	6	19,318	17,043	9	0	0	0	36,376
2.1-2.5	0	0	0	747	13,668	0	0	0	0	14,415
2.51-3	0	0	0	10	3,621	28	0	0	0	3,659
3.1-3.5	0	0	0	0	452	130	0	0	0	582
3.51-4	0	0	0	0	17	11	0	0	0	28
TOTAL	32	18,056	264,731	163,153	42,914	1,381	460	148	21	490,896

Table 5 Wave conditions for offloading operation

Displacements	Beam seas		Head seas		
	Safe offloading criteria	Operational	Safe offloading criteria	Operational-1	Operational-2
SURGE (X) (m)	0.031	0.041	0.105	0.462	0.578
SWAY(Y) (m)	0.366	0.829	3.00E-04	0.0003	0.0003
HEAVE(Z) (m)	0.692	1.443	0.249	0.517	0.646
ROLL (RX) (deg)	0.609	1.045	0.0004	0.0007	0.001
PITCH (RY) (deg)	0.27	0.369	0.674	1.505	1.882
YAW (RZ) (deg)	0.002	0.002	0.0006	0.0007	0.0008

Table 6 Cable response in different sea state

Cables	Beam seas		Head seas		
	Safe offloading criteria	Operational	Safe offloading criteria	Operational-1	Operational-2
1 (kN)	1010084.2	1131320.7	1010040.2	1129100.9	1128964.3
2 (kN)	1009812.4	1129191.0	1010107.0	1129149.5	1129012.7
3 (kN)	965760.4	1210000.2	965910.5	1210000.2	1210000.2
4 (kN)	965889.6	12100002.	965938.3	1210000.2	1210000.2
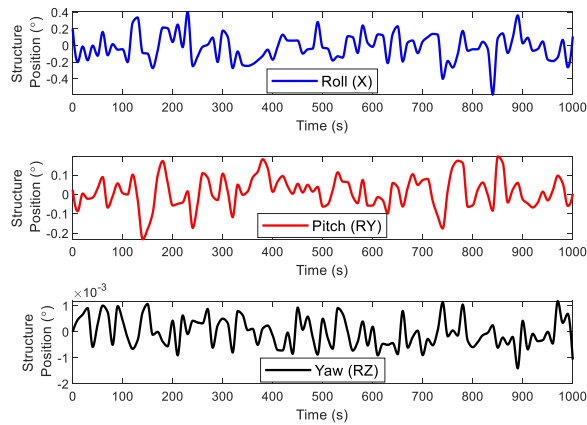
Fig. 6 Structure position (beam sea) - safe offloading criteria
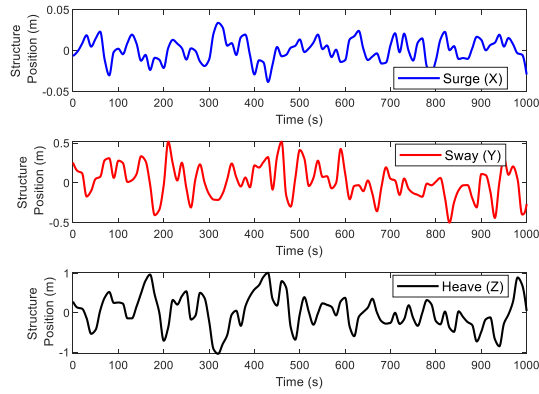
Fig. 7 Structure position (beam sea) - operational wave condition
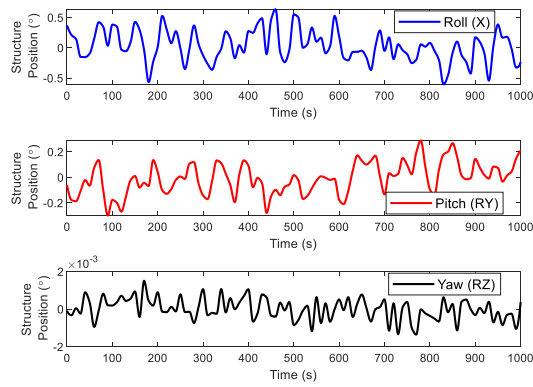
Fig. 8 Structure position (beam sea) - operational wave condition
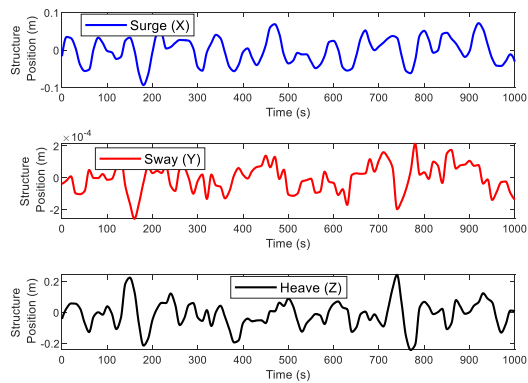
Fig. 9 Structure position (head sea) - safe offloading criteria

M.S. Patel et al.
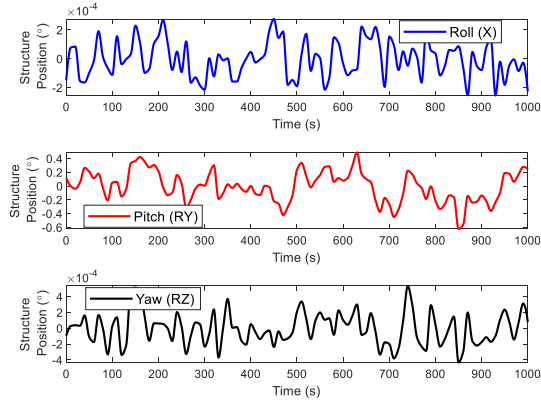
Fig. 10 Structure position (head sea) - safe offloading criteria
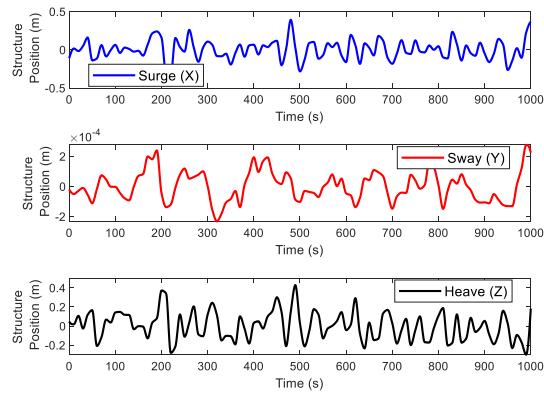
Fig. 11 Structure position (head sea) - operational wave condition 1
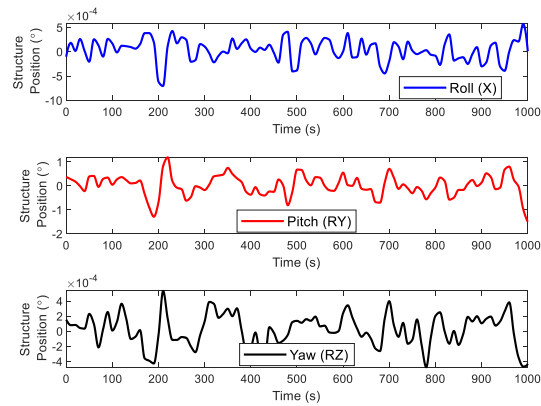
Fig. 12 Structure position (head sea) - operational wave condition 1
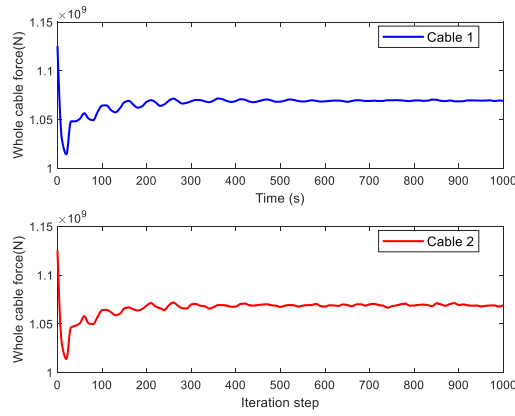
Fig. 13 Whole cable tensile force in beam sea - safe offloading criteria
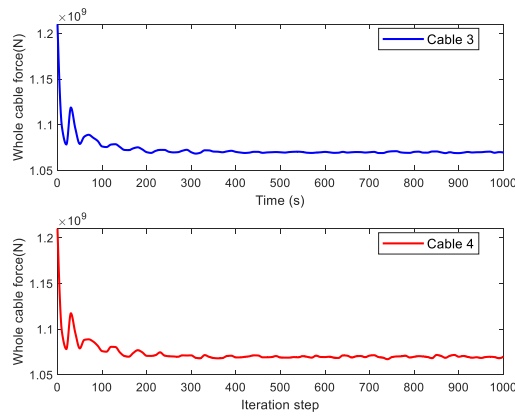
Fig. 14 Whole cable tensile force in beam sea - safe offloading criteria
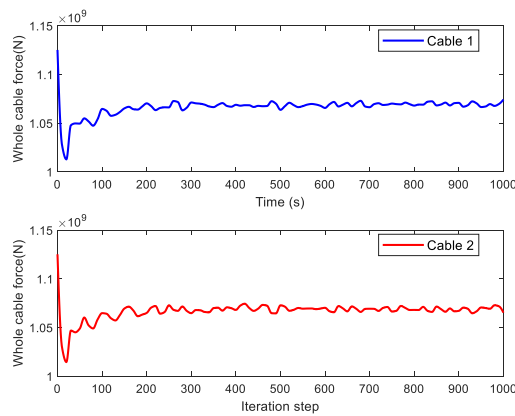
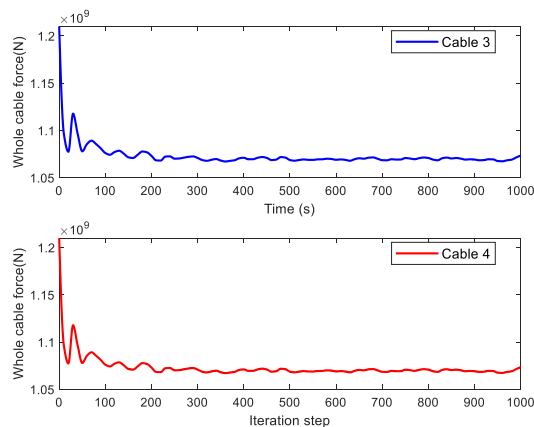Fig. 15 Whole cable tensile force in beam sea - operational wave condition
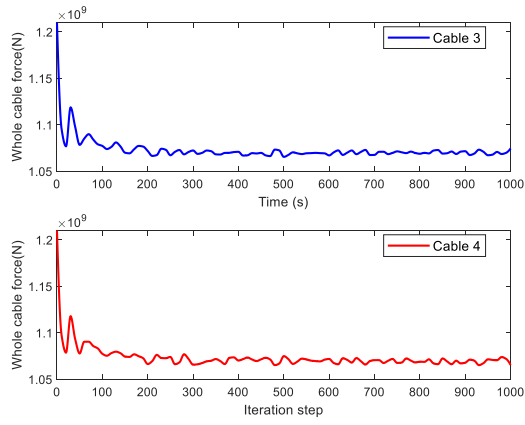
Fig. 16 Whole cable tensile force in beam sea - operational wave condition
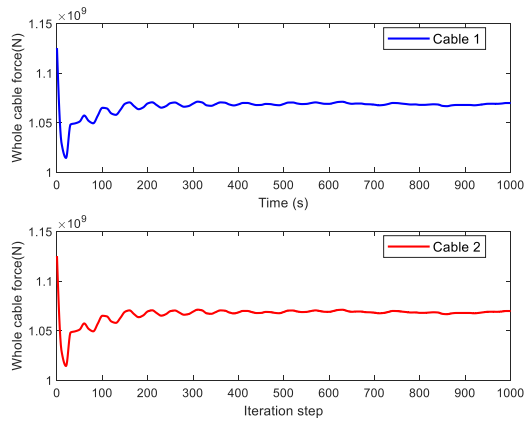
Fig. 17 Whole cable tensile force in head sea - safe offloading criteria
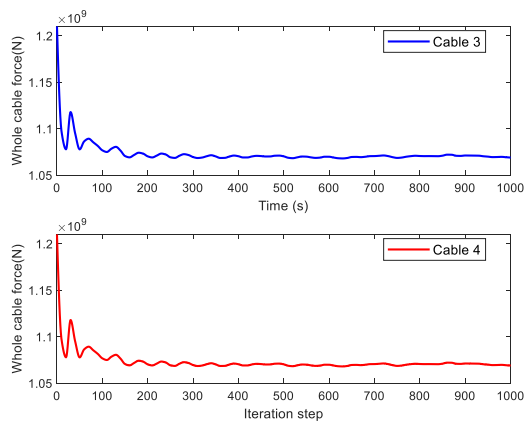
Fig. 18 Whole cable tensile force in head sea - safe offloading criteria
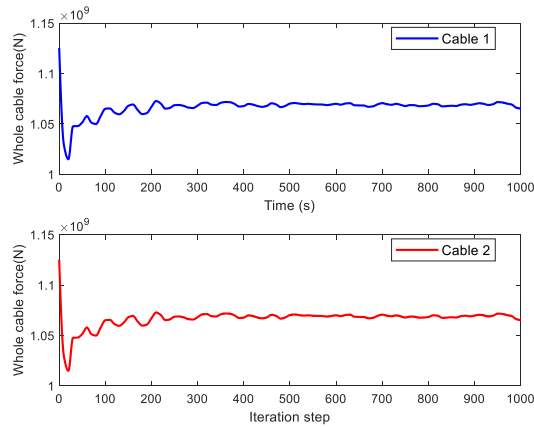
Fig. 19 Whole cable tensile force in head sea - operational wave condition 1

Fig. 20 Whole cable tensile force in head sea - operational wave condition 1

4.3 Mooring failure

The wave condition for simulating mooring failure is shown in Table 7. The two types of mooring failures are demonstrated here. Failure due to tension exceedance was simulated under beam sea state while single point failure was simulated under head sea state. In either cases of mooring failure, the whole cable forces under operational wave conditions exceeded the values under criteria wave condition. The failure of cable due to tension exceedance was simulated for cable 4 in beam seas. The failure of cable 4 takes place when it exceeds predefined tension of 965889.6 kN. The predefined tension was the value as obtained under safe offloading criteria. The single point failure was simulated for cable 3 in head seas. The cable was voluntarily made to fail at 200 seconds. The whole cable tensile response of the cables was observed when Cable 3 fails at 200 seconds. The behaviour of cables 1,2 and 3 in beam sea due to failure of cable 4 are shown in Figs. 21 and 22.

Table 7 Wave conditions for mooring failure

Sea-state	Wave condition
Beam sea	H_s = 2.0 m and T_p = 7.0 s
Head sea	H_s = 2.5 m and T_p = 7.0 s

The failure under head seas are shown in Figs. 23 and 24. It was observed that there was initial transient response at time of cable failure. The cable failure in beam sea caused instant increase in the whole cable tensile forces for the adjacent cable. There was shift in vibration about a new mean position for cable 3. Also, due to higher cable forces in the stern of FPSO, there was subsequent reduction in the whole cable forces 1 and 2 situated at bow of the FPSO, possible indication of slack in it. Overall transient response was observed for all the other cables at the time of failure of cable 4. The trend of response due to cable failure in head seas displayed similar behaviour.

5. Downtime cost analysis

The downtime cost analysis has been performed for offloading operations due to excursion of structure and whole cable response. Additionally, the downtime cost was also calculated due to failure of moorings. The probability of occurrence of operational wave conditions were determined from the wave scatter diagram. The downtime cost chart was represented with respect to the number of downtime days and also with respect to the percentage offloading capacity of shuttle tanker. The range of downtime days considered are 1, 2 and 3 days. The production capacity of FPSO is 318,000 barrels per day. Table 8 and 9 displays the considered inputs for the downtime cost analysis.
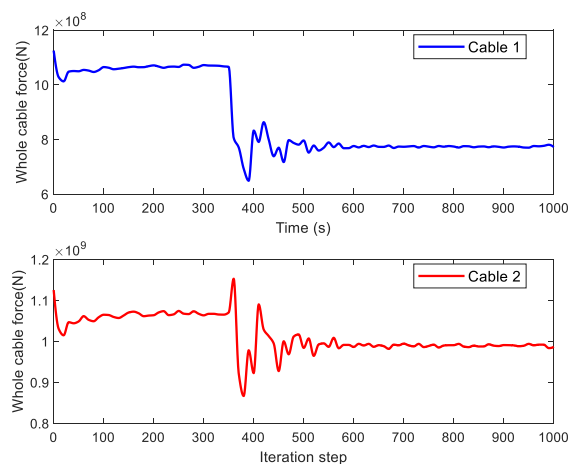

Fig. 21 Whole cable force in beam sea due to mooring failure

5.1 Downtime cost due to structure motion and cable excursion

The downtime cost is more proportional to the probability of occurrence and downtime days, since the OPEX and range of downtime days are same for all the operational wave conditions. In the beam sea, the probability of occurrence was highest for location 'A' while location 'B' has the minimum chance of occurrence.

Table 8 Particulars of downtime cost analysis for structure and cable responses

Beam sea (operational wave condition)			
Particulars	Location A	Location B	Location C
Probability occurrence	15.96%	4.99%	14.4%
OPEX (US$/barrel of oil)	35	35	35
Downtime day	1, 2, 3	1, 2, 3	1, 2, 3
Head sea (operational wave condition 1)			
Particulars	Location A	Location B	Location C
Probability occurrence	4.08%	2.88%	3.345%
OPEX (US$/barrel of oil)	35	35	35
Downtime day	1, 2, 3	1, 2, 3	1, 2, 3
Head sea (operational wave condition 2)			
Particulars	Location A	Location B	Location C
Probability occurrence	0.154%	1.21%	0.21%
OPEX (US$/barrel of oil)	35	35	35
Downtime day	1, 2, 3	1, 2, 3	1, 2, 3

Table 9 Particulars of downtime cost analysis for mooring failure

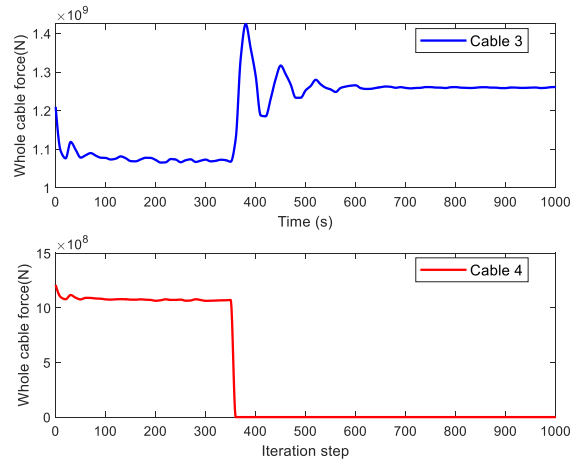| Beam sea			
Particulars	Location A	Location B	Location C
Probability occurrence	4.08%	2.88%	3.34%
OPEX (US$/barrel of oil)	35	35	35
Downtime day	1, 2, 3	1, 2, 3	1, 2, 3
Head sea			
Particulars	Location A	Location B	Location C
Probability occurrence	0.154%	1.21%	0.21%
OPEX (US$/barrel of oil)	35	35	35
Downtime day	1, 2, 3	1, 2, 3	1, 2, 3

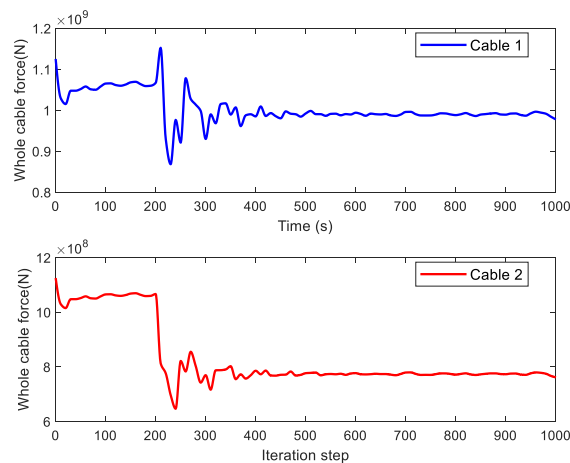Fig. 22 Whole cable force in beam sea due to mooring failure

Fig. 23 Whole cable force in head sea due to mooring failure

In head seas, the first operational wave conditions have the highest chance of occurrence in location 'A' and the second operational wave condition in location 'B'. The downtime cost charts were presented with respect to the variation in the offloading capacity of shuttle tanker. The downtime cost was calculated in million US\$. The downtime cost chart for second operational wave condition in head seas are displayed in appendix section of the paper. The downtime for offloading operations due to structure response excursion are displayed form Figs. 25 to 30. It is observed that the amount of downtime cost increases with the higher offloading capacity of shuttle tanker. The maximum downtime cost obtained in US\$ 5 million, US\$ 1.5 million and nearly US\$ 5 million for location 'A', 'B' and 'C', respectively for 3 downtime days, considering the highest offloading capacity in beam seas.
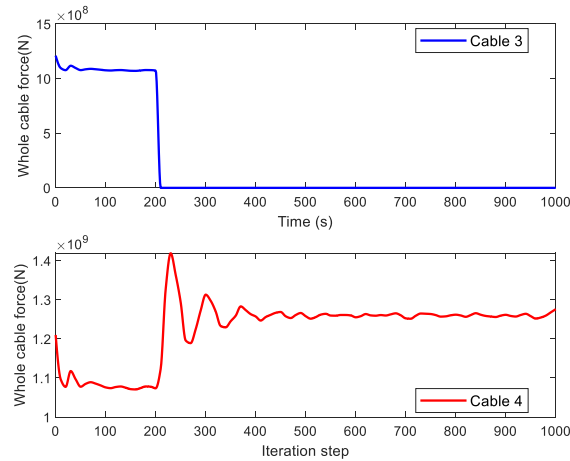
Fig. 24 Whole cable force in head sea due to mooring failure

Also, downtime cost was highest for location 'A' in beam sea-sate. Among all the considered offloading capacities in location 'A', the average per day downtime cost is nearly US$ 1.5 million. While location 'B' and 'C' has an average downtime cost of half million and nearly one million US$ per day. The downtime cost in head seas were not much impacted due to lower probability of occurrence. Out of the three considered location, the downtime cost was as high as US$ 1.4 million. Furthermore, the difference between the wave height of safe offloading criteria and operational wave condition in beam sea or head is 0.5 m. An unexpected increase in the wave height by small amount can significantly impact the global production costs.

5.2 Downtime cost due to failure of mooring cable

Since the wave condition for mooring failure under head sea was same as second operational wave condition, the downtime cost chart was the same in both the case. Therefore, the downtime cost charts due to mooring failure in beam sea are only presented. Figs. 31 to 33 displays the downtime cost chart of offloading operations due to mooring failure in beam sea. The probability of occurrence was highest for location 'A' and therefore the downtime cost was 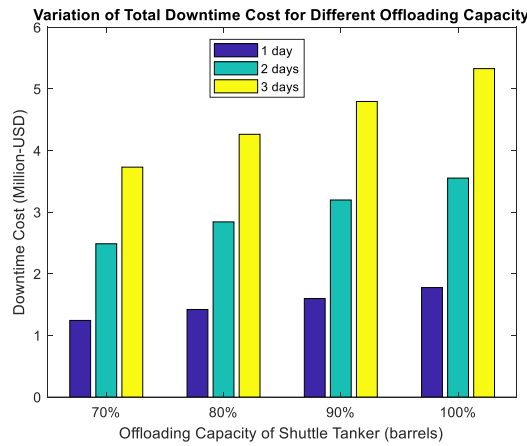maximum for it as compared to other two locations. For location 'A', the downtime cost to be faced by field operators for 70% offloading capacity ranges from US$ 0.3 million per day to nearly US$ 1 million per 3 days. There is marginal difference in the downtime cost between 80% and 90% offloading capacities. However, it varied from as low of nearly 0.4 million US$ per day to as high as close to US$ 1.2 million for 3 downtime days, respectively. In case of 100% offloading capacity, the maximum downtime cost incurred was close to US$ 1.4 million for 3 days. The maximum downtime cost in location `B' was close to US$ 1 million for 3 days while location 'C' suffered a downtime cost of slightly more than US$ 1 million for 3 downtime days.

Also, downtime cost was highest for location 'A' in beam sea-sate. Among all the considered offloading capacities in location 'A', the average per day downtime cost is nearly US$ 1.5 million. While location 'B' and 'C' has an average downtime cost of half million and nearly one million US$ per day. The downtime cost in head seas were not much impacted due to lower probability of

occurrence. Out of the three considered location, the downtime cost was as high as US$ 1.4 million. Furthermore, the difference between the wave height of safe offloading criteria and operational wave condition in beam sea or head is 0.5 m. An unexpected increase in the wave height by small amount can significantly impact the global production costs.

5.2 Downtime cost due to failure of mooring cable

Since the wave condition for mooring failure under head sea was same as second operational wave condition, the downtime cost chart was the same in both the case. Therefore, the downtime cost charts due to mooring failure in beam sea are only presented. Figs. 31 to 33 displays the downtime cost chart of offloading operations due to mooring failure in beam sea. The probability of occurrence was highest for location 'A' and therefore the downtime cost was maximum for it as compared to other two locations.

Fig. 25 Downtime cost for location A (beam sea)
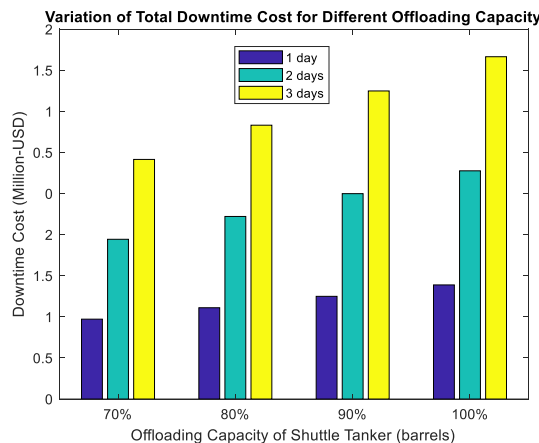
Fig. 26 Downtime cost for location B (beam sea)

Variation of Total Downtime Cost for Different Offloading Capacity
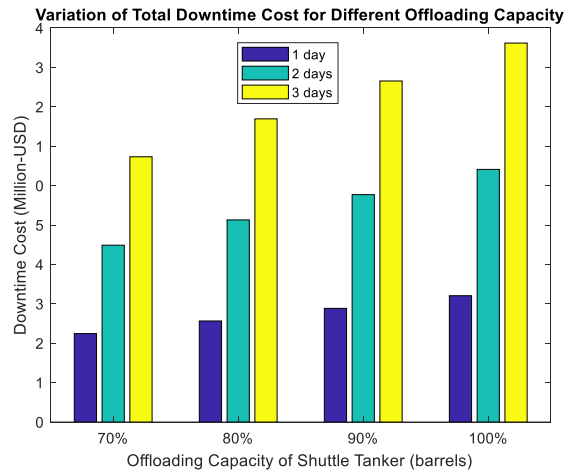
Fig. 27 Downtime cost for location C (beam sea)

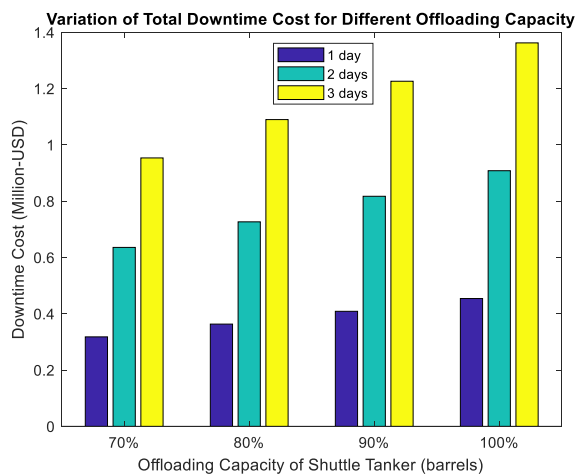**Variation of Total Downtime Cost for Different Offloading Capacity**

Fig. 28 Downtime cost for location A (head sea)

For location 'A', the downtime cost to be faced by field operators for 70% offloading capacity ranges from US$ 0.3 million per day to nearly US$ 1 million per 3 days. There is marginal difference in the downtime cost between 80% and 90% offloading capacities. However, it varied from as low of nearly 0.4 million US$ per day to as high as close to US$ 1.2 million for 3 downtime days, respectively. In case of 100% offloading capacity, the maximum downtime cost incurred was close to US$ 1.4 million for 3 days. The maximum downtime cost in location `B' was close to US$ 1 million for 3 days while location 'C' suffered a downtime cost of slightly more than US$ 1 million for 3 downtime days.

M.S. Patel et al.

Variation of Total Downtime Cost for Different Offloading Capacity

Fig. 29 Downtime cost for location B (head sea)

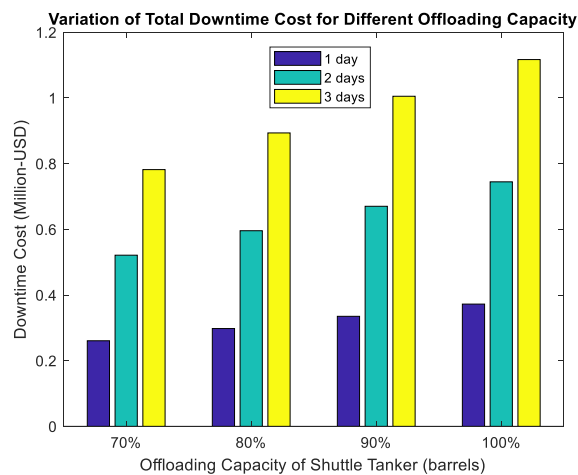**Variation of Total Downtime Cost for Different Offloading Capacity**

Fig. 30 Downtime cost for location C (head sea)

6. Conclusions

This study presented the downtime cost when wave conditions exceed the safe offloading criteria in Malaysian waters. An attempt to study the field downtime production cost of side-by-side offloading operations was discussed. The FPSO was numerically simulated in a time domain tool to study the excursion of motion and cable response when subjected to wave conditions greater than that for safe offloading criteria. Also, failure of mooring was simulated under wave conditions which exceed the safe offloading criteria. It can be concluded that beam sea-state was more critical in terms of the downtime cost due to motion and cable responses excursion.

Variation of Total Downtime Cost for Different Offloading Capacity
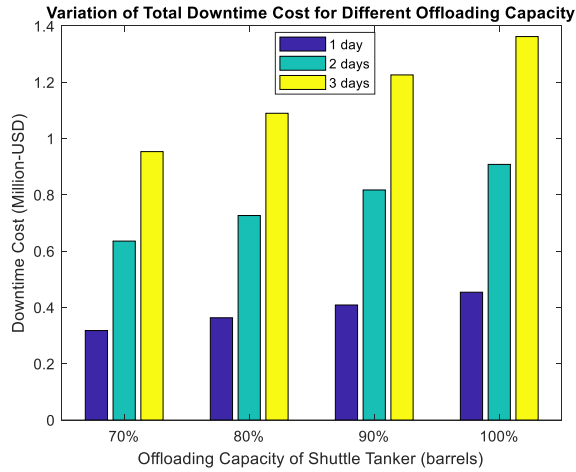
Fig. 31 Downtime cost due to mooring failure for location A (beam sea)

Variation of Total Downtime Cost for Different Offloading Capacity
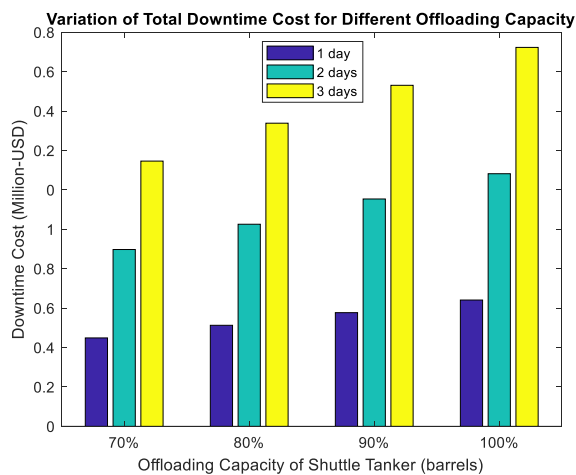

Fig. 32 Downtime cost due to mooring failure for location B (beam sea)

The field operators in location `A' would be most severely impacted with downtime cost between 1 million US$ to near about 5 million US\$ under beam seas. Comparatively, the heading seas did not contribute much to the downtime cost since probability of occurrence of operational wave conditions were less. The failure of mooring would affect the economic performance of the FPSO, and the production would maximum suffer a downtime cost of 1.3 million US$ per 3 days for location 'A' and more or less near 1 million US$ for locations 'B' and 'C'. It was seen that an unpredictable increase in the wave height by small amount of 0.5 m can affect the field operators drastically. However, the actual field downtime cost can be realistically evaluated if the OPEX is known.

The scope for future work includes development of Graphical User Interface (GUI) to evaluate the downtime cost of offloading operations.
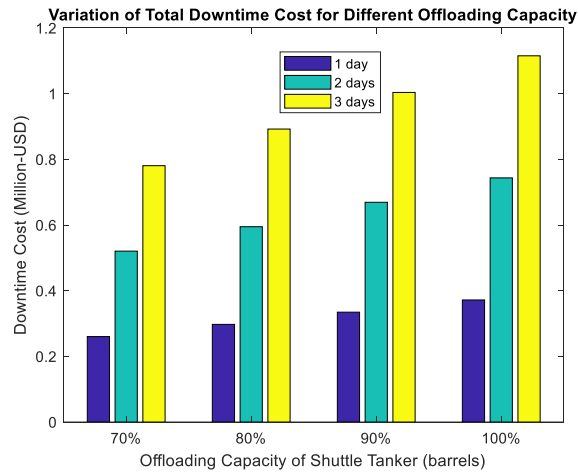
Fig. 33 Downtime cost due to mooring failure for location C (beam sea)

Acknowledgments

References

Ballard, E. and Evans, M. (2014), "Use of sequential downtime analysis in planning offshore operations", *Proceedings of the Annual Offshore Technology Conference* 2 (March): 1323–31.

Buchner, B., van Dijk, A. and de Wilde, J. (2001), "Numerical multiple-body simulations of side-by-side mooring to an FPSO", *Proceedings of the 11th International Offshore and Polar Engineering Conference*, 343–53.

Chang, Y., Chen, G., Zhang, L., Liu, X. and Liu, K. (2014), "Calculation and analysis of operability envelopes for deepwater drilling riser system", *Proceedings of the Annual Offshore Technology Conference* 2, 923-929.

Corrêa, D.C., De Oliveira, A.C., Tannuri, E.A. and Sphaier, S.H. (2013), "Comprehensive downtime analysis of Dp-assisted offloading operation of spread moored platforms in Brazilian waters", *Proceedings of the International Conference on Offshore Mechanics and Arctic Engineering - OMAE* 1 (2013), 7-9. https://doi.org/10.1115/OMAE2013-10405.

Cueva, M., *et al.* (2009), "Downtime analysis for offloading operation: DP x Non-DP shuttle tanker", 1-10.

Dqg, Huwk, Rzqwlph Xh, W R Lq, Wissanu Hattha, Tetsuya Hiraishi, Rdglqj Dqg, Xqordglqj Rshudwlrq, et al. (2017), "Berth operability and port downtime due to MetOCean in Eastern Thailand".

Ewans, Kevin C., and Phil Jameson. (2015), "Availability of offloading from an LNG Barge", *Appl. Ocean Res.*, **51**, 268-278. https://doi.org/10.1016/j.apor.2015.01.006.

Hong, S.Y., Kim, J.H., Kim, H.J. and Choi, Y.R. (2002), "Experimental study on behavior of tandem and side-by-side moored vessels", *Proceedings of the 12th International Offshore and Polar Engineering Conference* 3: 841-847.

Jin, C. and Kim, M.H. (2017), "Dynamic and structural responses of a submerged floating tunnel under extreme wave conditions", *Ocean Syst. Eng.*, **7**(4), 413-433. https://doi.org/10.12989/ose.2017.7.4.413.

Kessel-cobelens, Anneke M Van, Arianne P Verhagen, Jan M Mens, Chris J Snijders, and Bart W Koes (2008), "Methodology to determine floating LNG tank capacity by combination of side-by-side down-time simulatio on and cost/benefit analysis", no. September, 130-136. https://doi.org/10.1016/j.jmpt.2007.12.003.

Kim, H.C. and Kim, M.H. (2016), "Comparison of simulated platform dynamics in steady/dynamic winds and irregular waves for OC4 semi-submersible 5MW wind-turbine against deepCwind model-test results", *Ocean Syst. Eng.*, **6**(1), 1-21. https://doi.org/10.12989/ose.2016.6.1.001.

Lee, J.Y., Jin, C. and Kim,M.H. (2017), "Dynamic response analysis of submerged floating tunnels by wave and seismic excitations", *Ocean Syst. Eng.*, **7**(1), 1-19. https://doi.org/10.12989/ose.2017.7.1.001.

Lim, J.S., Muda, A.R., Razali, W., Sidek, M.S. and Hashim, A.F. (2015), "Redevelopment of brownfield in Malaysian offshore industry: A cost-optimized and mitigated-risk approach", *Society of Petroleum Engineers - Abu Dhabi International Petroleum Exhibition and Conference, ADIPEC 2015*.

Mahlstedt, B. and Davis, D. (2017), "Worldwide Survey of Floating Production, Storage and Offloading (FPSO) Units", *Offshore Magazine*.

Morandini, C., Legerstee, F. and Mombaerts, J. (2002), "Criteria for analysis of offloading operation", *Proceedings of the Annual Offshore Technology Conference*, 2751-2755.

Nishanth, R. (2018), "Dynamic Response and Life-Cycle Analysis of Floating Production Storage and Offloading Systems", no. October.

Nishanth, R., John, V.K. and Whyte, A. (2016), "Dynamic behaviour of FPSO in Kikeh field under different loading conditions", *ARPN J. Eng. Appl. Sci.*, **11**(4), 2302-2307.

Paquet, S., Lamourette, E., Auburtin, E., Hellesmark, S.B. and Thorsen, T.B. (2016), "Safe LNG loading of conventional LNG carriers in severe open sea environments", *Proceedings of the Offshore Technology Conference Asia 2016, OTCA 2016*, 3813-3835.

Patel, M.S., Liew, M.S., Mustaffa, Z., Al-Yacouby, A.M., Said Abdurrasheed, A. and Whyte,A. (2019), "Downtime cost analysis of offloading operations considering vessel motions and mooring responses in Malaysian waters", *Proceedings of the 2019 IEEE Student Conference on Research and Development, SCOReD 2019*, no. 1: 63-68. https://doi.org/10.1109/SCORED.2019.8896325.

Patel, M.S., Liew, M.S., Mustaffa, Z., Yee, N.C. and Whyte, A. (2020), "Development of downtime cost calculator for offloading operations influenced by parametric rolling", *J. Mar. Sci. Eng.*, **8**(1). https://doi.org/10.3390/JMSE8010007.

Peng, H. and Spencer, D. (2008), "Simulation of dynamic positioning of a FPSO and a shuttle tanker during offloading operation", *Proceedings of the International Offshore and Polar Engineering Conference* 8, 148-153.

Pillay, A., Wang, J., Wall, A.D. and Ruxton, T. (2001), "A maintenance study of fishing vessel equipment using delay-time analysis", *J. Quality in Maint. Eng.*, **7**(2), 118-127. https://doi.org/10.1108/13552510110397421.

Poldervaart, L., Oomen, H. and Ellis, J. (2006), "Offshore LNG transfer: A worldwide review of offloading availability", https://doi.org/10.4043/18026-ms.

Patel M.S., Liew, M.S., Mustaffa, Z., Abdurrasheed, S.A. and Whyte, A. (2020), "Effects of Motion Responses and Drift Forces on Side-by-Side Offloading Operations of FPSO", *Advancement in Emerging Technologies and Engineering Applications*, no. 1: 407-413. https://doi.org/https://doi.org/10.1007/978-981-15-0002-2_43.

Van Doorn, J.T.M. and ten Hove, D. (2002), "F(P)SO offloading concepts, their nautical feasibility and safety assessment", *Proceedings of the Annual Offshore Technology Conference*, 2623-2630.

Zhao, W., Yang, J. and Hu, Z. (2012), "Hydrodynamic Interaction between FLNG Vessel and LNG Carrier in Side by Side Configuration", *J. Hydrodynamics* **24**(5), 648-657. https://doi.org/10.1016/S1001-6058(11)60288-6.

Zhao, W., Pan, Z., Lin, F., Li, B., Taylor, P.H. and Efthymiou, M. (2018), "Estimation of gap resonance relevant

to side-by-side offloading", *Ocean Eng*., **153**, 1-9. https://doi.org/10.1016/j.oceaneng.2018.01.056.
Zhao, W., Yang, J., Hu, Z. and Tao, L. (2014), "Prediction of hydrodynamic performance of an FLNG system in   side-by-side   offloading   operation",   *J.   Fluids   Struct*.,   **46**,   89-110. https://doi.org/10.1016/j.jfluidstructs.2013.11.021.

MK

Appendix

This section includes all the results including the down time cost charts under head seas for operational wave condition H_s=2.5 m and T_p=8 s. Figs. 34 to 40 are the results for second operational wave condition in head seas.
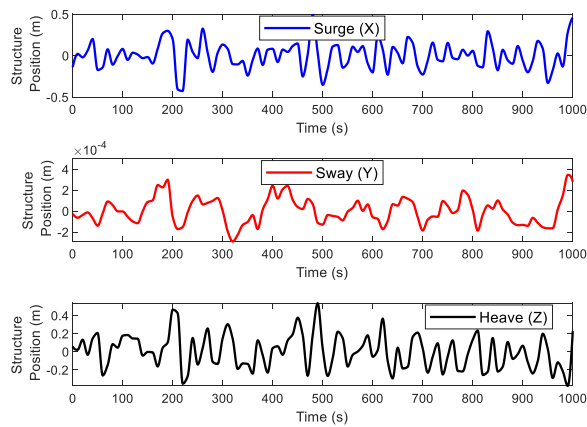
Fig. 34 Structure position (head sea) - operational wave condition 2
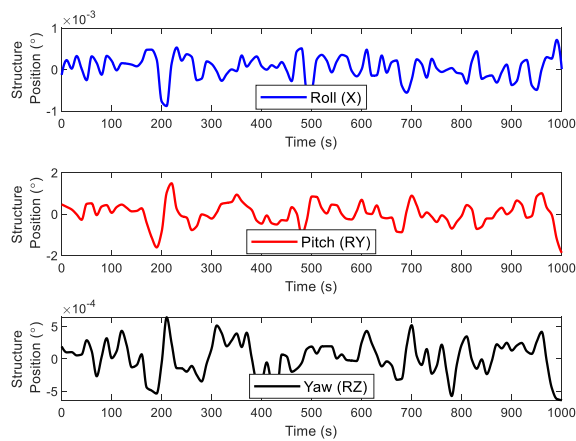
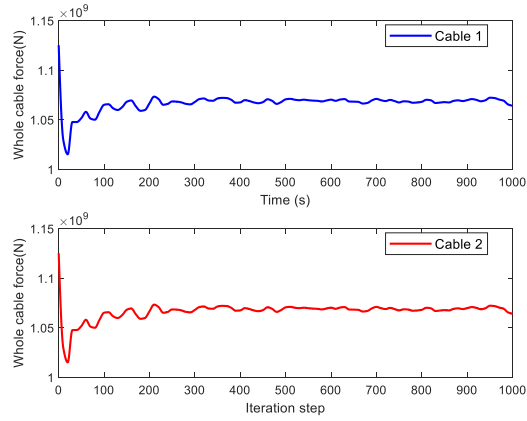Fig. 35 Structure position (head sea) - operational wave condition 2

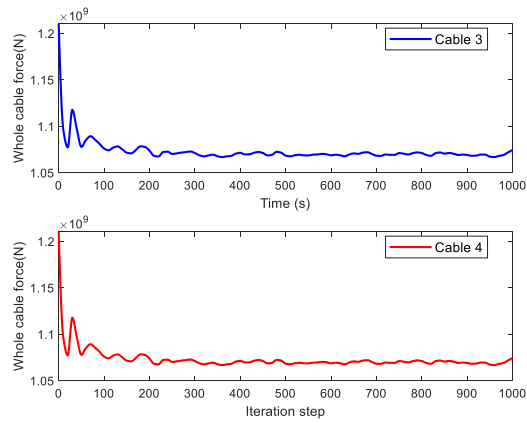Fig. 36 Whole cable tensile force in head sea - operational wave condition 2

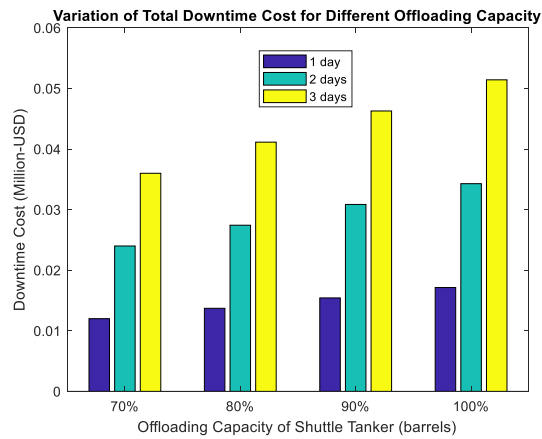Fig. 37 Whole cable tensile force in head sea - operational wave condition 2

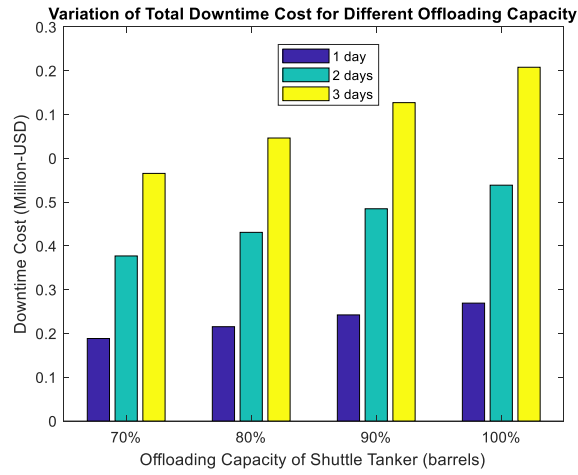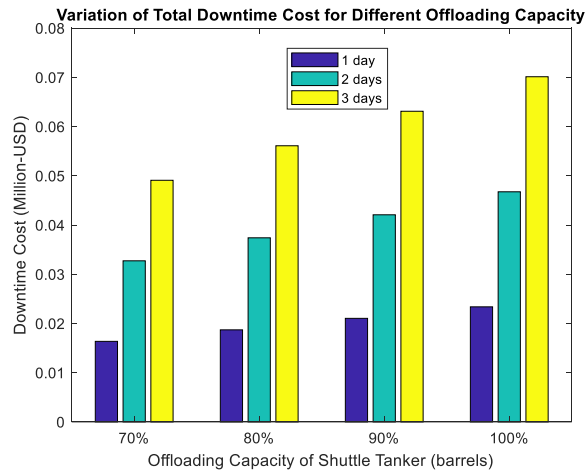Fig. 38 Downtime cost for location A (head sea)

Fig. 39 Downtime cost for location B (head sea)

Fig. 40 Downtime cost for location C (head sea)